Eur. Phys. J. D **37**, 157–162 (2006)
DOI: 10.1140/epjd/e2005-00258-6

THE EUROPEAN PHYSICAL JOURNAL D

Selective reflection by atomic vapor: experiments and self-consistent theory

A. Badalyan, V. Chaltykyan, G. Grigoryan, A. Papoyan[a], S. Shmavonyan, and M. Movsessian

Institute for Physical Research, NAS of Armenia, Ashtarak-2, 378410 Armenia

Received 27 June 2005 / Received in final form 1st August 2005
Published online 27 September 2005 – © EDP Sciences, Società Italiana di Fisica, Springer-Verlag 2005

Abstract. Selective reflection of laser radiation from the interface between atomic vapor and a dielectric is studied for a wide range of vapor density. A self-consistent model is developed, some analytical results are obtained, as well as a number of curves are computed that are in good agreement with experimental spectra measured in cesium and rubidium vapor cells.

PACS. 39.30.+w Spectroscopic techniques – 42.25.Gy Edge and boundary effects; reflection and refraction – 32.70.Jz Line shapes, widths, and shifts

1 Introduction

Reflection of radiation from the boundary between a dielectric and atomic vapor is termed as selective reflection (SR), because it has a prominent spectral structure on the atomic transition frequencies [1–3]. The selective reflection is an essential spectroscopic tool differing in a number of aspects from the absorption spectroscopy because of relatively narrow width of spectral lines. Among the applications of SR spectroscopy is: study of the van-der-Waals interaction of atoms with a dielectric surface [4], determination of the homogeneous width and the shift of resonance lines [5,6], of cross-sections of resonant collisions [7], narrowing of generation spectrum of broadband lasers, study of coherent and magneto-optical processes [8–10], locking a diode laser frequency to atomic resonance lines [11,12], etc. This technique may, in particular, be useful for the problems of determination of abundances of isotopes in natural atomic vapors.

The small widths of spectral lines in SR, resolving the resonances inside the Doppler profile, is associated with non-locality of the atomic medium polarization and with peculiarity of interaction of atoms having different velocity directions with the cell walls [2,13]. Indeed, the atoms lose their polarization in collisions with the cell wall. So, the induced dipole moment for the positive velocity atoms near the input window is equal to zero, while for negative velocity atoms it does not vanish. Near the output window the pattern is opposite. Such a selectivity of the polarization with respect to the sign of the velocity projection gives, as a result, the experimentally observed spectra. The polarization non-locality (spatial dispersion) is in this case displayed on the lengths of the order $\lambda\gamma_{Dop}/\gamma$ (λ is the wavelength of the incident radiation, γ_{Dop} the Doppler width, and γ the full homogeneous width, i.e., the sum of the natural and collisional self-broadening widths).

There are many theoretical and experimental studies of SR [7,14–24]. Theoretical models deal as a rule with the approximation of dilute media which is valid for only the densities of the resonant gas where the collision linewidth is much narrower than the Doppler broadening (see, e.g., [14,16,17,19,20]). Absorption of laser radiation is in this approach completely neglected.

In other limiting case of high densities when the collision broadening exceeds well the Doppler width, the spatial dispersion of the medium may be disregarded and the reflected signal is well described by the so-called quasi-stationary solution by means of the complex refraction index for a resonantly absorbing medium [25].

The general self-consistent problem of SR is, to the best of our knowledge, not yet solved, except for references [21,22], where it is treated numerically.

The present work is aimed at theoretical study of the selective reflection in atomic media with arbitrary optical density and detailed experimental investigations in cesium and rubidium vapor in a wide range of densities (from $\gamma_{Dop}/\gamma \ll 1$ up to $\gamma_{Dop}/\gamma \gg 1$). The intensity of laser radiation was being in these studies properly chosen to be sufficiently low (lower than 0.1 mW/cm^2 in the entire range of densities) as to avoid nonlinear effects such as saturation and optical pumping. The cell length was much longer than the length of linear absorption which allowed us to avoid interference effects, occurring in thin cells, that may affect essentially the shape of the reflected signal (see [17,20,23]). The theoretical model is based on the self-consistent solution of Maxwell equations together with the density matrix equation for a multilevel system. We obtain relatively simple expressions well describing the

[a] e-mail: papoyan@ipr.sci.am

experimental results and passing, in limiting cases, to the well-known ones; computed curves are in agreement with the results of measurements.

The theory is presented in Section 2. The experimental results and their comparison with the computed curves are given in Section 3.

2 Theory

We calculate as well as compute the selective reflection spectra for atomic vapor at various temperatures (atomic number densities). For this purpose we consider an one-dimensional problem where the laser radiation is assumed to be a monochromatic plane wave incident normally on the interface between the cell-window material and the resonant vapor. This wave is partially reflected from the window surface and partially transmitted through the vapor cell. So, we represent the electric field strengths of these three fields in the form

$$\begin{aligned} E_{inc} &= \mathrm{Re}\left\{\mathcal{E}_0 \exp(-i(\omega t - kn_1 x))\right\}, \\ E_{ref} &= \mathrm{Re}\left\{\mathcal{E}_R \exp(-i(\omega t + kn_1 x))\right\}, \\ E_{tr} &= \mathrm{Re}\left\{\mathcal{E}_T \exp(-i(\omega t - kn_3 x + \varphi))\right\}. \end{aligned} \tag{1}$$

Here $\varphi = kL(1-n_3)$, L is the length of the vapor column, $n_{1,3}$ are the refraction indices of respective media, $k = \omega/c$ (the phase φ is introduced for convenience). The field inside the resonant medium and the medium polarization may be written as

$$\begin{aligned} E_{med} &= \mathrm{Re}\left\{\mathcal{E}(x) \exp(-i\omega t)\right\}, \\ P_{med} &= \mathrm{Re}\left\{\mathcal{P}(x) \exp(-i\omega t)\right\}. \end{aligned} \tag{2}$$

The conditions of continuity of fields and of their derivatives on the interfaces read

$$\begin{aligned} &\mathcal{E}(0) = \mathcal{E}_0 + \mathcal{E}_R, && \mathcal{E}(L) = \mathcal{E}_T \exp(ikL), \\ &\frac{\partial \mathcal{E}(0)}{\partial x} = in_1 k\left(\mathcal{E}_0 - \mathcal{E}_R\right), && \frac{\partial \mathcal{E}(L)}{\partial x} = in_3 k \mathcal{E}_T \exp(ikL). \end{aligned} \tag{3}$$

The experimentally measured reflection coefficient is defined, according to (3), as

$$R = \left|\frac{\mathcal{E}_R}{\mathcal{E}_0}\right|^2 = \left|\frac{ikn_1\mathcal{E}(0) - \dfrac{d\mathcal{E}}{dx}(0)}{ikn_1\mathcal{E}(0) + \dfrac{d\mathcal{E}}{dx}(0)}\right|^2. \tag{4}$$

The field $\mathcal{E}$ should be calculated in a self-consistent way by solving the density matrix equations along with the Maxwell equations for the fields. We will consider the linear case (the input signal is weak), which makes possible to consider the multilevel system as a number of independent two-level atomic systems (i.e., the medium polarization may be represented as $P(x,u) = \sum\limits_n P_n(x,u)$; n being the numbers of the excited atomic levels). The system of Maxwell and density matrix equations is in this case reduced to

$$\begin{aligned} \frac{d^2\mathcal{E}(x)}{dx^2} + k^2\mathcal{E}(x) &= -4\pi k^2 \left\langle \mathcal{P}(x,u)\right\rangle_u, \\ u\frac{d\mathcal{P}_n(x,u)}{dx} + (\gamma_n - i\Delta_n)\mathcal{P}_n(x,u) &= i\frac{N(u)\mathcal{E}(x)}{\hbar}\left|d_n\right|^2. \end{aligned} \tag{5}$$

Here $N(u)$ is the number density of the ground-state atoms (with u being the atomic velocity projection on the light propagation direction), Δ_n, d_n are, respectively, the detuning of resonance and the atomic $1 \to n$ transition dipole moment, $\mathcal{P}_n = N(u)d_n\rho_{n1}$, ρ_{n1} the corresponding nondiagonal element of the density matrix, and γ_n is the full width of the transition: $\gamma_n = (1/2)\Gamma_{natural} + \Gamma_{collision} + \Gamma_{buffer} + \Gamma_{laser}$; $\langle ... \rangle_u$ means averaging over the (Maxwellian) velocity distribution (the quantity $\Gamma_{collision}$ is generally complex describing both the broadening and the shift).

The correct boundary conditions for the medium polarization are [16]

$$\mathcal{P}_n(x=0, u>0) = 0, \qquad \mathcal{P}_n(x=L, u<0) = 0. \tag{6}$$

We assume in what follows that the cell length L exceeds essentially the length of penetration and $\mathcal{E}_T$ in (3) may be set equal to zero.

From the second equation of the system (5) and the boundary conditions (6) we obtain for the polarization $\mathcal{P}_n$ (see, e.g. [22])

$$\begin{aligned} \mathcal{P}_n(x,u>0) &= i(q\beta_n/u)\int\limits_0^x \mathcal{E}(y) \\ &\quad \times \exp\left\{-(\gamma_n - i\Delta_n)\frac{x-y}{u}\right\} dy \\ \mathcal{P}_n(x,u<0) &= i(q\beta_n/u)\int\limits_L^x \mathcal{E}(y) \\ &\quad \times \exp\left\{-(\gamma_n - i\Delta_n)\frac{x-y}{u}\right\} dy. \end{aligned} \tag{7}$$

Here the following notations are introduced: $q = Nd^2/\hbar$, $\beta_n = |d_n|^2/d^2$ with $d^2 = \sum |d_n|^2$. By substituting (7) into the Maxwell equation and replacing $u<0$ by $-u>0$ we obtain the following equation:

$$\begin{aligned} &\frac{d^2\mathcal{E}(x)}{dx^2} + k^2\mathcal{E}(x) = \\ &\quad -4\pi k^2 iq\left\{\int\limits_0^x \mathcal{E}(y)\chi(x-y)\,dy + \int\limits_x^L \mathcal{E}(y)\chi(y-x)\,dy\right\}, \end{aligned} \tag{8}$$

where

$$\chi(x-y) = \sum_n \beta_n \left\langle \frac{1}{u}\exp\left\{-\frac{\gamma_n - i\Delta_n}{u}(x-y)\right\}\right\rangle_{u>0}.$$

The first integral in the *rhs* of the equation (8) is the macroscopic polarization caused by atoms with positive velocities, while the second one is caused by atoms with negative velocities. If we now replace x by $z = L - x$, we obtain a boundary problem for the function $\mathcal{E}_1(z) = \mathcal{E}(L - z)$ with zero initial conditions:

$$\frac{d^2\mathcal{E}_1(z)}{dz^2} + k^2\mathcal{E}_1(z) = -4\pi k^2 iq \left\{ \int_z^L \mathcal{E}_1(y)\chi(y-z)dy + \int_0^z \mathcal{E}_1(y)\chi(z-y)dy \right\} \tag{9}$$

$$\mathcal{E}_1(0) = 0; \quad \frac{d\mathcal{E}_1(0)}{dz} = 0.$$

In general case the solution to the problem (9) with the corresponding boundary conditions is rather complicated, but we will be interested in only the asymptotic values entering the expression (4)

$$\mathcal{E}_1(L \to \infty) = \mathcal{E}(0); \quad \frac{d\mathcal{E}_1}{dz}(L \to \infty) = -\frac{d\mathcal{E}}{dx}(0). \tag{10}$$

So, we only need to determine the asymptotic solution to the equation (9) at $L \to \infty$. It is easy to see that the contribution from the first integral in the *rhs* of (9) into the asymptotic solution goes to zero and we have

$$\frac{d^2\mathcal{E}_1}{dz^2} + k^2\mathcal{E}_1 = -4\pi k^2 iq \left\{ \int_0^z \mathcal{E}_1(y)\chi(z-y)dy \right\}. \tag{11}$$

By performing the Laplace transformation in (11) and using the convolution properties we obtain

$$\left(s^2 + k^2\right)\widetilde{\mathcal{E}}_1(s) = -4\pi k^2 iq\chi(s)\widetilde{\mathcal{E}}_1(s),$$
$$\widetilde{\chi}(s) = \sum_n \beta_n \left\langle \frac{1}{su + \gamma_n - i\Delta_n} \right\rangle_{u>0}. \tag{12}$$

The equation (12) has a unique solution only if the following condition is met:

$$s^2 + k^2 + 4\pi k^2 iq\widetilde{\chi}(s) = 0. \tag{13}$$

In general case it may easily be shown that the equation (13) has two roots, one of which is damping ($\mathrm{Re}(s) < 0$) and does not contribute to the asymptotic solution. So, we have finally

$$\mathcal{E}_1(z) = Ae^{pz}, \tag{14}$$

where p is that root of (13), which has a positive real part. So, the reflection coefficient acquires the form

$$R = \left| \frac{ikn_1\mathcal{E}_1(L) + \mathcal{E}_1'(L)}{ikn_1\mathcal{E}_1(L) - \mathcal{E}_1'(L)} \right|^2 = \left| \frac{ikn_1 + p}{ikn_1 - p} \right|^2,$$
$$p = -ik\sqrt{1 + 4\pi X} \tag{15}$$

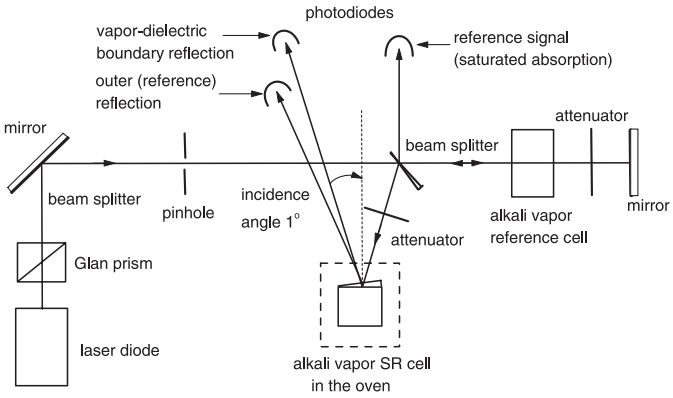

Fig. 1. Schematic drawing of the experimental set-up.

(the choice of p is caused by the condition $\mathrm{Re(p)} > 0$) or

$$R = \left| \frac{n_1 - \sqrt{1 + 4\pi X}}{n_1 + \sqrt{1 + 4\pi X}} \right|^2. \tag{16}$$

The quantity X in these expressions is the polarizability of the resonant medium, which is determined by the equation

$$X = -q \sum_n \beta_n \left\langle \frac{1}{ku\sqrt{1 + 4\pi X} + \Delta_n + i\gamma_n} \right\rangle_{u>0}. \tag{17}$$

Note that in dilute media ($q \ll 1$) the reflection coefficient may be expanded into a series with respect to q; the first term of this expansion gives the well-known expression (see, e.g., [17,16]). The opposite limiting case of dense media gives for the quantity X the following expression

$$X = -q \sum_n \beta_n \frac{1}{\Delta_n + i\gamma_n}. \tag{18}$$

In general case a simple iteration procedure may be used providing the expression for the reflection coefficient to any desired accuracy:

$$X_k = -q \sum_n \beta_n \left\langle \frac{1}{ku\sqrt{1 + 4\pi X_{k-1}} + \Delta_n + i\gamma_n} \right\rangle_{u>0}. \tag{19}$$

In the case of a two-level system equation (17) reduces to a cubic equation that may be solved with use of the Cardano formulas.

3 Experimental results and discussion

In this section we report the experimental studies of the selective reflection covering a wide range of atomic number densities from the dilute to dense vapor limiting cases.

Schematic diagram of the experimental set-up is shown in Figure 1. Standard free running diode lasers (spectral linewidth $\Delta\nu_L \sim 20$ MHz) were used as a tunable radiation source in the range of the D lines of atomic cesium and rubidium. A fraction of the laser radiation was branched

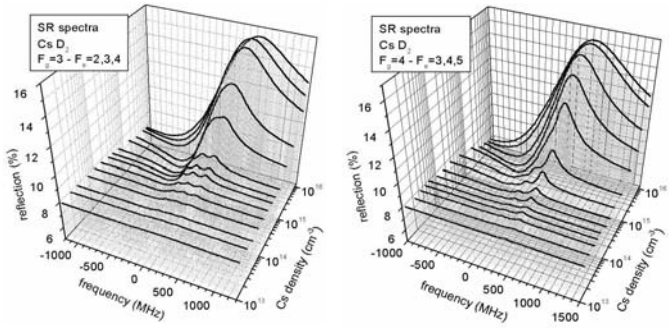

Fig. 2. Vapor density dependence of selective reflection spectra for $F_g = 3 \rightarrow F_e = 2, 3, 4$ and $F_g = 4 \rightarrow F_e = 3, 4, 5$ transition groups of Cs D_2 line.

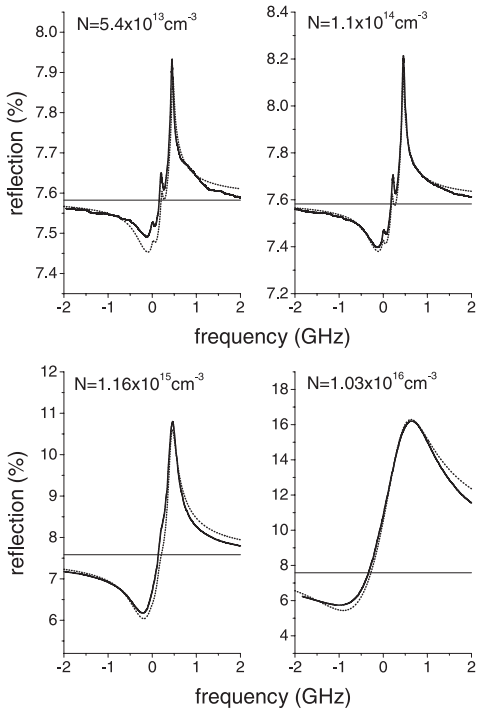

Fig. 3. Experimental (solid lines) and theoretical (dotted lines) selective reflection spectra for $F_g = 4 \longrightarrow F_e = 3, 4, 5$ transitions of Cs D_2 line at various number densities of atomic vapor. Horizontal line shows the value of off-resonance reflection.

to an auxiliary saturated absorption (SA) set-up to have a frequency reference. The main, linearly polarized radiation beam, of 2–3 mm diameter, was directed nearly normally (the incidence angle ∼20 mrad) onto the front sapphire window of the SR glass cell with the side-arm containing alkali metal. The cell was placed in a two-section oven, which allowed one to individually control the temperatures of the cell body and of the side arm. The power of the incident beam was attenuated to typically 20 μW to avoid the saturation and optical pumping effects. The reflected radiation power was detected by a photodiode placed 1 m away from the window. At this distance the beam spots reflected from the outer and inner faces of the slightly wedged front window are completely separated. Small detection solid angle of the SR signal (0.0001 srad) allowed us to suppress the resonance fluorescence contribution to the recorded signal. The SR and SA photodiodes were provided by operation amplifiers and followed by a DAQ board allowing two-channel computer recording and processing of the signals.

To obtain SR spectra, the laser radiation frequency was linearly scanned up to $\Delta\nu_{scan} = 20$ GHz through the spectral region covering the chosen groups of hyperfine transitions of given alkali D line. The scanning was realized by application of periodical triangular pulses with 5 s typical rise/fall time. Each spectrum contained 1000 acquired points with 50 measurements per point.

In the T-shaped sealed-off cells we used, the saturated vapor pressure is determined by a side arm reservoir temperature T_{sa} (more precisely, temperature of the metal-vacuum boundary, the coldest spot in the cell). The window temperature T_w has to be set to somewhat higher value for preventing vapor condensation; the value of T_w does not affect significantly the atomic vapor density N. The latter was determined using Langmuir-Tailor equations [26].

The regular measurements were done at various temperature conditions, for ∼50 values of N ranged between 10^{12} and 5×10^{16} cm^{-3}. The SR spectra were recorded after complete stabilization of the temperature regimes, as monitored by thermocouple gauges. The minimum value of N was chosen so that to ensure acceptable signal to noise ratio for direct recording (no frequency modulation) of the SR spectra; the maximum value of N employed was limited by operation temperature conditions in the cells. Note that the above-mentioned density range covers the entire region of passage from dilute to dense vapor, as defined in Section 2.

Figure 2 shows the general evolution of the SR spectra with number density of atoms for the case of Cs D_2 line, separately for $F_g = 3 \rightarrow F_e = 2, 3, 4$ and $F_g = 4 \rightarrow F_e = 3, 4, 5$ transitions. The SR spectra exhibit well pronounced sub-Doppler structure at low vapor densities, which is not clearly visible in Figure 2 because of the same scale for all the plots. Increase of N results in growth of the sub-Doppler peak amplitudes without noticeable increase of their linewidths (dilute vapor regime, $N \lesssim 5 \times 10^{14}$ cm^{-3}). As vapor density rises, the increase of peak amplitudes is accompanied by broadening of the structure (intermediate regime, $N \sim 5 \times 10^{14}$–10^{16} cm^{-3}). The further increase of N causes essential broadening of the SR signal (the sub-Doppler structure is washed out), while the growth of signal amplitudes saturates (dense vapor regime, $N \gtrsim 10^{16}$ cm^{-3}).

The experiment with rubidium was done using the cells filled with natural mixture of ^{85}Rb and ^{87}Rb isotopes (abundances, respectively, 72.2% and 27.8%). Accordingly, the low density D_1 line SR spectra consist of 8 sub-Doppler peaks (transitions $F_g = 2, 3 \rightarrow F_e = 2, 3$ of ^{85}Rb and $F_g = 1, 2 \rightarrow F_e = 1, 2$ of ^{87}Rb), and the D_2

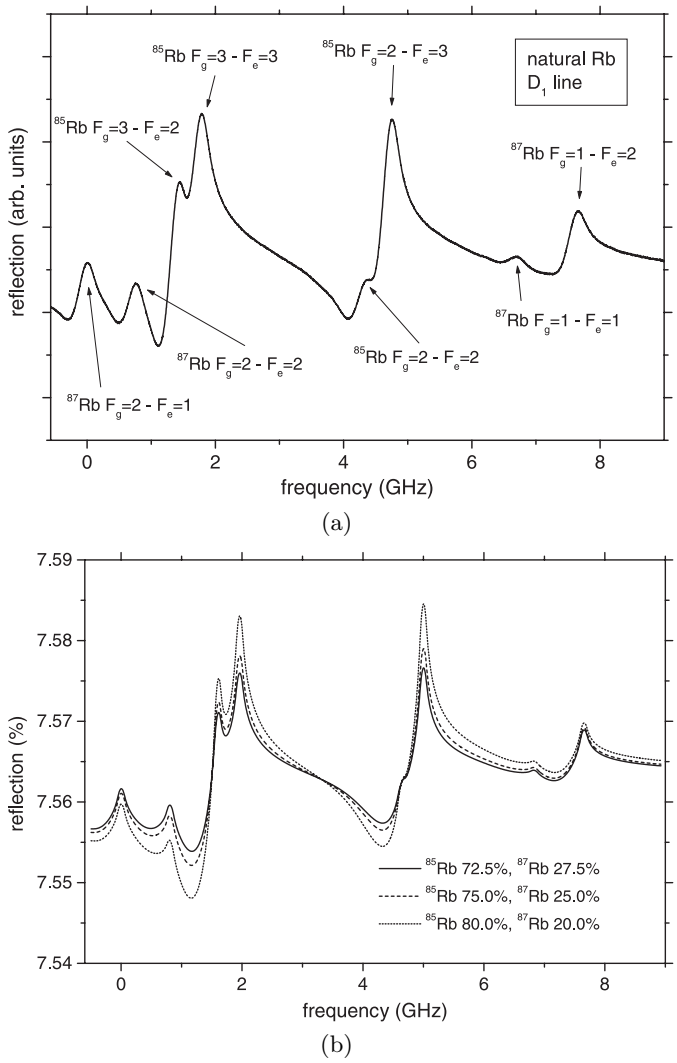

Fig. 4. Selective reflection spectra for D_1 line of Rb: (a) experimental curve for natural rubidium; (b) calculated curves for various isotopic abundances. The vapor density is $N = 10^{14}$ cm^{-3}.

line spectra consist of 12 sub-Doppler peaks (transitions $F_g = 2 \to F_e = 1, 2, 3$; $F_g = 3 \to F_e = 2, 3, 4$ of ^{85}Rb and $F_g = 1 \to F_e = 0, 1, 2$; $F_g = 2 \to F_e = 1, 2, 3$ of ^{87}Rb).

Figure 3 demonstrates the comparison of some experimentally obtained SR spectra with those computed by means of formulas (16) and (19) for the D_2 line of cesium. In calculations we added the Lorentz-Lorenz shift (see, e.g., [22]) into the expression (19). The iteration series converges sufficiently fast, so computed were actually the first three terms. The values of all the parameters needed for computations were taken from reference [26]. The plots show a good agreement between the calculations and measurements.

SR spectrum for the D_1 line of natural rubidium measured at the vapor density of about 10^{14} cm^{-3} is shown in Figure 4a. The same spectrum calculated theoretically is given in Figure 4b at three different abundances of ^{85}Rb and ^{87}Rb. It is well seen that a change in the abundance of one of isotopes leads to a drastical modification of the SR spectrum. This means that SR measurements can serve as a sensitive and visualizing tool for determination of percentage of isotopes in mixtures.

4 Conclusion

The selective reflection of laser radiation from the interface between atomic vapor and cell window is studied theoretically and experimentally. A theoretical self-consistent model is developed, valid for arbitrary vapor densities. Simple expressions are obtained enabling one to calculate the SR spectra to the needed accuracy. A number of selective reflection spectra were recorded in Cs and Rb vapors under various experimental conditions; in particular, the vapor density in the cells was varied in a wide range from 10^{12} to 10^{17} cm^{-3}. At low densities the spectra exhibit prominent sub-Doppler structure, while at high densities ($\sim 5 \times 10^{15}$ cm^{-3}) the structure practically disappears. The amplitude of the reflection signal saturates at densities higher than 10^{16} cm^{-3}. Analytical calculations as well as numerical simulations based on suggested theoretical model explaining these peculiarities, are in good agreement with the experimental results in the entire density range.

This work was supported, in part, by the ISTC grant #A-635.

References

1. R.W. Wood, Philos. Mag. **18**, 187 (1909)
2. J.L. Cojan, Ann. Phys. (Paris) **9**, 385 (1954)
3. J.P. Woerdman, M.F.H. Schuurmans, Opt. Commun. **14**, 248 (1975)
4. M. Chevrollier, M. Fichet, M. Oriá, G. Rahmat, D. Bloch, M. Ducloy, J. Phys. II France **2**, 631 (1992)
5. V. Vuletić, V.A. Sautenkov, C. Zimmermann, T.W. Hänsch, Opt. Commun. **99**, 185 (1993)
6. A.V. Papoyan, J. Contemp. Phys. (Arm. Acad. Sci.) **33**, 8 (1998)
7. A.V. Papoyan, G.S. Sarkisyan, S.V. Shmavonyan, Opt. Spectrosc. **85**, 649 (1998)
8. A. Weis, V.A. Sautenkov, T.W. Hänsch, Phys. Rev. A **45**, 7991 (1992)
9. B. Gross, N. Papageorgiou, V.A. Sautenkov, A. Weis, Phys. Rev. A **55**, 2973 (1997)
10. N. Papageorgiou, A. Weis, V.A. Sautenkov, D. Bloch, M. Ducloy, Appl. Phys. B **59**, 123 (1994)
11. R. Müller, A. Weis, Appl. Phys. B **66**, 323 (1998)
12. R.N. Li, S.T. Jia, D. Bloch, M. Ducloy, Opt. Commun. **146**, 186 (1998)
13. M.F.H. Schuurmans, J. Phys. (Paris) **37**, 469 (1976)
14. J. Guo, J. Cooper, A. Gallagher, M. Lewenstein, Opt. Commun. **110**, 197 (1994)
15. M. Chevrollier, M. Oriá, J.G. de Souza, D. Bloch, M. Fichet, M. Ducloy, Phys. Rev. E **63**, 046610 (2001)

16. T.A. Vartanyan, F. Träger, Opt. Commun. **110**, 315 (1994); T.A. Vartanyan, D. Lin, Phys. Rev. A **51**, 1959 (1995)
17. G. Dutier, S. Saltiel, D. Bloch, M. Ducloy, J. Opt. Soc. Am. B **20**, 793 (2003)
18. T.A. Vartanyan, Zh. Eksp. Teor. Fiz. **88**, 4 (1985)
19. V.A. Sautenkov, V.L. Velichansky, A.S. Zibrov, V.N. Lukyanov, Kvant. Elektron. **8**, 1867 (1981)
20. B. Zambon, G. Nienhuis, Opt. Commun. **143**, 308 (1997)
21. P. Wang, A. Gallagher, J. Cooper, Phys. Rev. A **56**, 1598 (1997)
22. J. Guo, J. Cooper, A. Gallagher, Phys. Rev. A **53**, 1130 (1996)
23. A.V. Papoyan, G.G. Grigoryan, S.V. Shmavonyan, D. Sarkisyan, J. Guena, M. Lintz, M.A. Bouchiat, Eur. Phys. J. D **30**, 265 (2004)
24. G. Nienhuis, F. Schuller, M. Ducloy, Phys. Rev. A **38**, 5197 (1988)
25. Y.L. Welch, I. Kastner, A.C. Lauriston, Can. J. Res. A **28**, 93 (1950)
26. D.A. Steck, Cs D line data; Rb 87 D line data, `http://steck.us/alkalidata`